The influence of groundwater representation on hydrological simulation and its assessment using satellite-based water storage variation

Zhongwei Huang[1,5], Qiuhong Tang[1,5*], Min-Hui Lo[2], Xingcai Liu[1], Hui Lu[3], Xuejun Zhang[1] and Guoyong Leng[4]

[1]Key Laboratory of Water Cycle and Related Land Surface Processes, Institute of Geographic Sciences and Natural Resources Research, Chinese Academy of Sciences, Beijing 100101, China

[2]National Taiwan University, Department of Atmospheric Sciences, Taipei 10617, Taiwan

[3]Ministry of Education Key Laboratory for Earth System Modeling, and Center for Earth System Science, Tsinghua University, Beijing, 100084 China

[4]Joint Global Change Research Institute, Pacific Northwest National Laboratory, College Park MD 20740, USA

[5]University of Chinese Academy of Sciences, Beijing 100049, China

Emails: Zhongwei Huang (huangzw.14b@igsnrr.ac.cn); Qiuhong Tang (tangqh@igsnrr.ac.cn); Min-Hui Lo (minhuilo@ntu.edu.tw); Xingcai Liu (xingcailiu@igsnrr.ac.cn); Hui Lu (luhui@tsinghua.edu.cn); Xuejun Zhang (zhangxj.13b@igsnrr.ac.cn); Guoyong Leng (Guoyong.Leng@gmail.com)

[*]*Corresponding author*: Qiuhong Tang (Tel: +86-10-6488-9722 Email: tangqh@igsnrr.ac.cn)

This article has been accepted for publication and undergone full peer review but has not been through the copyediting, typesetting, pagination and proofreading process which may lead to differences between this version and the Version of Record. Please cite this article as doi: 10.1002/hyp.13393

Abstract. The interaction between surface water and groundwater is an important aspect of hydrological processes. Despite its importance, groundwater isn't well represented in many land surface models (LSMs). In this study, a groundwater module with consideration of surface water and groundwater dynamic interactions is incorporated into the Distributed Biosphere Hydrological (DBH) model in the upstream of the Yellow River basin, China. Two numerical experiments are conducted using the DBH model: one with groundwater module active, namely DBH_GW and the other without, namely DBH_NGW. Simulations by two experiments are compared with observed river discharge and terrestrial water storage (TWS) variation from the Gravity Recovery and Climate Experiment (GRACE). The results show that river discharge during the low flow season that is underestimated in the DBH_NGW has been improved by incorporating the groundwater scheme. As for the TWS, simulation in DBH_GW shows better agreement with GRACE data in terms of inter-annual and intra-seasonal variations and annual changing trend. Furthermore, compared with DBH_GW, TWS simulated in DBH_NGW shows smaller decreases during autumn and smaller increases in spring. These results suggest that consideration of groundwater dynamics enables a more reasonable representation of TWS change by increasing TWS amplitudes and signals, and as a consequence, improves river discharge simulation in the low flow seasons when groundwater is a major component in runoff. Additionally, incorporation of groundwater module also leads to wetter soil moisture and higher evapotranspiration (ET), especially in the wet seasons.

Key words: Groundwater; hydrological simulation; DBH model; river discharge; terrestrial water storage

1 Introduction

Groundwater interacts with soil moisture under gravity and capillary forces, and exchanges with water in river channels under hydraulic head gradient. These interactions are key land surface processes and have significant impacts on the land surface energy and water balance ((Liang et al., 1994; Maxwell & Miller, 2005; Niu et al., 2007; Wada et al., 2010). Groundwater dynamics are considerable factor for runoff generation, and further influence the volumes and variations of streamflow in river channels, especially in temperate zones where subsurface flow or baseflow from deep soil moisture and groundwater accounts for a large proportion of total runoff (Cherkauer & Lettenmaier, 1999; Lam et al., 2011). Furthermore, the interaction between groundwater and surface water is likely to affect the soil moisture in unsaturated zones, thus further affect evapotranspiration (ET) (Sellers, 1986; Liang et al., 2003; Shiklomanov & Rodda, 2004; Fan et al., 2007; Pokhrel et al., 2013; Lin et al., 2016).

Over the past few decades, land surface models (LSMs), which are applied to quantitatively represent the fluxes of radiation, water vapor, heat, and momentum across the land and atmosphere interface, have evolved from the simple, unrealistic schemes into reasonable representations of the soil-vegetation-atmosphere system (Sellers, 1986; Liang et al., 1994; Sellers et al., 1996; Tang & Oki, 2016). However, the absence of groundwater module or the poor parameterization of interactions between surface water and groundwater is still an open issue for most of LSMs (Zeng et al., 2016). Alkama et al. (2010) pointed out that the lack of groundwater parameterization is one main culprit of overestimation of annual

river discharge and underestimation of continental ET by LSMs. Zhang et al. (2014) illustrated that the Variable Infiltration Capacity (VIC) model tends to underestimate streamflow in the dry season across the river basins over northern China, because groundwater is the main source of river baseflow in dry seasons due to its long response time and water memory effect. Cai et al.(2014) analyzed that unconfined aquifer storage layer for groundwater dynamics is of great significance to hydrological modeling for major hydrological variables (e.g. runoff, ET, and soil moisture).

The need for a groundwater module in LSMs has received increasing attention in the past decade, and some studies have incorporated groundwater schemes into LSMs ((Arora & Boer, 1999; Alcamo et al., 2003; Maxwell & Miller, 2005; Niu et al., 2007; Lo et al., 2008; Fan et al., 2013; Leng et al., 2014). Liang et al. (2003) reported that incorporating a groundwater scheme into VIC model would result in drier soil in upper layer and wetter soil in lower layer, thus leading to lower surface runoff peaks, higher base flow and less ET in two watersheds in Pennsylvania, USA. By incorporating the water table dynamics into a LSM, Yeh and Eltahir (2005) represented that the simulation of soil water budget and river discharges gained great improvments in Illinois, especially in low flow seasons. Niu et al. (2007) reported that a simple groundwater scheme (SIMGM) in a LSM will produce much wetter soil and larger evapotranspiration for the global as a whole than that by without groundwater representation, most obviously in arid-to-wet transition regions. Ferguson and Maxwell (2010) demonstrated that feedbacks between groundwater and land surface water and energy balance would greatly effect the hydrologic sensitivity to climate change by using a LSM with groundwater module. Miguez-Macho et al.(2012 a,b) concluded that

groundwater reservoir may be an important regulator of the Amazon water cycle both for water and energy balance, and the potential mechanism of the interactions between surface water and groundwater water were further analyzed based on model simulation. In general, emerged from previous studies on the role of groundwater dynamics on hydrological simulations is that groundwater regulates seasonal pattern of soil moisture and river discharge by its low frequency variations and delayed response to precipitation.

However, it is difficult to evaluate the role of groundwater module in a LSM due to lack of water table or soil moisture observations (Vergnes & Decharme, 2012). Fortunately, the advent of NASA's Gravity Recovery and Climate Experiment (GRACE) satellite mission provides the opportunity for large-scale measurements of TWS variation. TWS, including water stored as soil moisture, snow and ice, groundwater, lakes and rivers, and the water contained in biomass, interacts with other terrestrial and meteorological factors to shape climate and control weather (Rodell & Famiglietti, 2001). Previous studies have demonstrated the possibility of using GRACE data to estimate the TWS variations (Rodell & Famiglietti, 2001; Niu et al., 2007; Lo et al., 2010; Pokhrel et al., 2013). Groundwater is a considerable component of the TWS (Miguez-Macho & Fan, 2012; Pokhrel et al., 2013; Leng et al., 2014), and the inter-annual variability or trend of TWS may not be consistent with the GRACE measurements without considration of groundwater component (Decharme et al., 2010; Döll et al., 2014). It is therefore possible to use the TWS measurements from GRACE for evaluate the add-value of groundwater representation in LSMs on TWS simulation.

This study uses the framework of the Distributed Biosphere-Hydrological (DBH) model to investigate the role of groundwater dynamics on water budget at large scale, especially to

correct underestimation of streamflow during the winter season, and further to assess the add-value of inclusion of the groundwater dynamics on TWS variation using GRACE estimates. In this paper, section 2 introduces the model and the groundwater scheme. Section 3 describes the study region, model parmeters and experiment design. The influences of the groundwater scheme on the hydrological simulations are analyzed in section 4. Key mechanism of the impacts of groundwater representation and possible limitions of groudwater module and potential future works are discussed in section 5. Conclusion is given in section 6.

2 Model descriptions

2.1 The DBH model

The DBH model, which couples the revised Simple Biosphere (SiB2) model (Sellers et al., 1996) with a distributed hydrological model, can be used to simulate the transfer of energy and water between atmosphere and land surface (Tang et al., 2006). The model has been widely used in many studies (Davie et al., 2013; Hattermann et al., 2016; Liu et al., 2016). In the following, the processes related to soil water fluxes and runoff generation in the DBH model are briefly described.

The model without a groundwater module is denoted as DBH_NGW. A 3-layer model (Fig. 1(a)) is adopted to calculate hydraulic diffusion and gravitational drainage of water in the soil. Soil water fluxes between layers are derived using Darcy's law:

$$q_{i,i+1} = K_{i,i+1}\left(\frac{\partial \psi_{i,i+1}}{\partial z_{i,i+1}} + 1\right), \text{ for } i = 1,2 \qquad (1)$$

where $q_{i,i+1}$ is vertical water exchange between soil layers (m s^{-1}), $K_{i,i+1}$ is the hydraulic conductivity between soil layers (m s^{-1}), $\psi_{i,i+1}$ is soil moisture potential between soil layers (m), and $z_{i,i+1}$ is vertical distance (m). The hydraulic conductivity K and soil moisture potential ψ of three soil layers are calculated by the water-retention equation of Brooks and Corey (1966):

$$\psi = \psi_{sat}(\frac{\theta}{\theta_{sat}})^{-b}$$

$$K = K_{sat}(\frac{\theta}{\theta_{sat}})^{(2b+3)/b}, \quad (2)$$

where ψ_{sat} is saturation soil moisture potential (m); K_{sat} is saturation hydraulic conductivity (m s^{-1}); θ_{sat} is the soil water content at saturation (i.e., porosity); θ is the soil water content (%); b is the empirical soil pore size distribution index.

The baseflow Q_b from the recharge zone (Layer 3) is determined by the gravitational drainage and the heterogeneities in soil moisture fields (Sellers et al., 1996):

$$Q_b = f_{ice}(K_{sat}W_3^{(2b+3)}\sin\phi + 0.001\frac{\theta_{sat}D_3W_3}{T}), \quad (3)$$

Where the factor f_{ice} allows for a progressive reduction in soil hydraulic conductively as the soil freezes and it is defined in Sellers et al. (1996); W_3 is the soil wetness of Layer 3 (m^3/m^3); ϕ is the average slope angle; D_3 is the thickness of Layer 3 (m); and T is the time step (second).

2.2 Groundwater scheme

A simple groundwater scheme is developed by adding an extra layer in the 3-layer model of DBH, which connects soil layers and groundwater reservoir. The model with the groundwater scheme is denoted as DBH_GW, which can well represent the interactions among groundwater, soil moisture, and water in river channels (Fig. 1(b)). The upper boundary of the added layer is soil in Layer3, while the lower boundary is the water table. Thus, he transfer of water between groundwater and the third layer is given by:

$$q_{3g} = K_{3g}\left(\frac{\partial \psi_{3g}}{\partial z_{3g}} + 1\right) \quad , \tag{4}$$

where q_{3g} is the vertical water interaction between the third soil layer and groundwater; ψ_{3g} is soil moisture potential (m); z_{3g} is vertical distance (m); K_{3g} is the effective hydraulic conductivity between the third soil layer and the groundwater table, estimated as:

$$K_{3g} = f_{ice}\left[\frac{K_3\psi_3 - K_{sat}\psi_{sat}}{\psi_s - \psi_3}\right]\left[\frac{b}{b+3}\right] \quad . \tag{5}$$

The baseflow from soil follows the ARNO model conceptualization (Todini, 1988; Franchini & Pacciani, 1991), which is applied only to the third soil layer to depict the nonlinear process of baseflow recession. Base flow from the third soil layer is given by:

$$Q_{b1} = \begin{cases} \frac{D_s D_m}{W_s W_{3c}} W_3, 0 \le W_3 \le W_s W_{3c} \\ \frac{D_s D_m}{W_s W_{3c}} W + (D_m - \frac{D_s D_m}{W_s})(\frac{W_3 - W_s W_{3c}}{W_{3c} - W_s W_{3c}})^2, W_3 \ge W_s W_{3c} \end{cases} \quad , \tag{6}$$

where Q_{b1} is the subsurface runoff from soil (mm/day); W_3 is the soil moisture wetness of the third soil layer (m^3/m^3); D_m is the maximum subsurface flow under saturation (mm/day); D_s

is the fraction of D_m where non-linear (rapidly increasing) baseflow begins; W_{3c} is the maximum soil moisture wetness of the third soil layer (m^3/m^3); W_s is the fraction of W_{3c} where non-linear baseflow begins, with $D_s<W_s$.

The representation of river-groundwater exchange is considered to be groundwater flow into a river over a sloping impermeable river bed (Childs, 1971; Towner, 1975), which can be expressed with the absolute slope of the water table and the hydraulic conductivity (Tang et al., 2007):

$$Q_{b2} = K_s h_g \left(\frac{dh_g}{ds}\cos\theta_b + \sin\theta_b\right) \quad , \tag{7}$$

where Q_{b2} is the flow between the groundwater and river water (m^2/s); θ_b is the bed slope (rad); s is the distance along the riverbed (m); and hg is the aquifer thickness (m). $\frac{dh_g}{ds}$ is calculated as: $\frac{dh_g}{ds} = \frac{h_r \cos\theta_b - h_w}{L/2\cos\theta_b}$, where h_r is the depth of river; h_w is the groundwater level; and L is the width of hillslope which is set as half of the value of grid area to river length in the grid cell. $Q_{b2}>0$ indicates that water flows from groundwater to river network, while $Q_{b2}<0$ means river recharge groundwater (see Figure S1).

Change in groundwater depth Δh_w is calculated by the groundwater reservoir storage variation:

$$\frac{\Delta h_w}{\Delta t} = \frac{(q_{3g} - Q_{b2} - Q_l)}{\mu}, \tag{8}$$

where Q_l is groundwater discharge in water depth by other reasons (e.g. groundwater extraction by human) (m/s); μ is the specific yield with μ=0.1 is used in this study.

3 Study region and experiments

3.1 Study region

Both DBH_NGW and DBH_GW are applied in the upstream of the Yellow River basin above the Tangnaihai station (Fig. 2). The area of the study region is 117,524 km^2, which accounts for 16.2% of the total area of the Yellow River basin. The study area is in the Northeast Tibet Plateau with a high elevation between 2670 and 6250m, and has a typically plateau climate. Annual average air temperature varies between -4℃ and 2℃ from northwest to southeast. While mean annual precipitation for the period of 1982–2014 is 488 mm, with 70-90% of rainfall occurring in the wet seasons (June to September) due to the southwest monsoon from the Indian Ocean (Tang et al., 2008). Grassland covers about 80% of the study area, and only grazing activities occurs there. The upstream of the Yellow River basin is selected for two reasons: firstly, there are very few human activities (e.g. irrigation and reservoirs) and can be treated as unimpaired (Cong et al., 2009); secondly, the study region is a typical arid-to-wet transition region where groundwater discharge is the main component of runoff, especially in dry seasons and groundwater dynamics also have large impacts on water and energy balance.

3.2 Datasets

The meteorological forcing data from 36 meteorological stations within and close to the study area are obtained from the China Meteorological Administration (CMA) over the period from 1982 to 2014 (http://data.cma.cn/). This data includes the daily precipitation, mean air temperature, maximum and minimum air temperature, mean surface relative humidity, sunshine duration and wind speed. The station datasets are then spatially interpolated to 10×10 km grids using an inverse-distance weighted method, wherein the interpolation of air temperature considered the effects of elevation (New et al., 2000; Yang et al., 2006). The vegetation condition forcing data, leaf area index (LAI) and fraction of photosynthetically active radiation (FPAR) absorbed by the green vegetation canopy are obtained from Boston University (Myneni et al., 1997; Zhu et al., 2013). The vegetation condition indices were also resampled to the 10×10 km grids. The observed monthly discharge over 2003-2014 at Tangnaihai station, which are applied for model calibration and validation, was obtained from Ministry of Water Resources of China (Information Center of Water Resources, 2003-2014).

The latest GRACE Tellus land products (RL05) provided by the Center for Space Research (CSR), Geo Forschungs Zentrum Potsdam (GFZ), and Jet Propulsion Laboratory (JPL) are used (https://grace.jpl.nasa.gov/data/get-data/). The GRACE data, which estimates the monthly variation of TWS, is at a spatial resolution of 1°×1°. The spatial average values of GRACE data in the upstream of the Yellow River basin are estimated using a mask which is derived from the DEM of the study region, and used to extract the values of three GRACE products from 1°×1° spatial resolution. Due to the post-processing and sampling of GRACE data, TWS variations at grid scale tend to be adjusted by multiplying scaling factors first that

are derived from the Community Land Model (CLM4.0) (Landerer & Swenson, 2012). In this study, gridded scaling factors provided together with the GRACE Tellus products were applied to these three GRACE data. We use these three data sets from 2003 to 2014 (excluding the missing data in June 2003, January 2011, June 2011, May 2012, October 2012, March 2013, August 2013, September 2013, February 2014 and December 2014; the missing data was filled using linear interpolation method). Since the GRACE TWS data are anomalies relative to the 2004-2009 time-mean base-line, we also compute the anomalies of TWS for model simulations based on the 2004–2009 average TWS. As all three centers produced reasonably similar TWS anomalies for the period of 2003 to 2014, the ensemble mean of these three GRACE products were obtained for evaluation.

3.3 Parameters and model calibration

The soil parameters, such as the soil water potential at saturation ψ_{sat} (m), soil hydraulic conductivity at saturation *Ks* (m s^{-1}), soil pore size distribution index *b*, and porosity θ_{sat}, were derived from the Food and Agriculture Organization Digital Soil Map of the World. The configuration of the three soil layers for both DBH_GW and DBH_NGW is 0.02, 0.78, and 0.2 meters for the surface layer, root zone and recharge layer, respectively. The parameters, including the precipitation heterogeneity parameters P_a, P_b, and P_c (Tang et al., 2007) in both DBH_GW and DBH_NGW, and the ARNO model parameters D_s and W_s only in DBH_GW were calibrated, and then the simulated streamflow was validated against the monthly discharge from 2003 to 2014 at Tangnaihai station. In DBH model, the precipitation heterogeneity parameters P_a, P_b, and P_c are applied to represent the effects of sub-grid heterogeneity in precipitation on hydrological processes. Consistent with previous

study (Tang et al., 2007), we set P_a=P_b, and P_c=e^{Pa}, and the precipitation variability within a grid cell will become larger with increasing P_a. In model calibration (in DBH_NGW), P_a was set between 2 to 10 at the interval of 0.5, and 17 runs of simulations were conducted for the period 1982-2014. In order to remove the effects due to uncertain initial conditions, the 1982-2002 period is treated as spin-up, and the remaining 12 years (2003-2014) of simulation were used for validations. For each run, the simulated monthly streamflow is compared with observations, and the P_a, P_b, and P_c that maximize the Nash-Sutcliffe efficiency coefficient (NSC) between simulated and observed monthly streamflow are chose as the optimal values. Here parameters are set as P_a=P_b=5.5 for optimal configuration for DBH_NGW. To make equal comparisons between DBH_GW and DBH_NGW, the precipitation heterogeneity parameters were set to P_a=P_b=5.5 in both DBH_GW and DBH_NGW. The parameters D_s and W_s that govern subsurface runoff process in DBH_GW are calibrated to be 0.002 and 0.6, respectively, using the same calibration methods as for P_a and P_b. Therefore, both DBH_NGW and DBH_GW are calibrated against observations, and the input data (e.g. climate data and soil parameters) and the precipitation heterogeneity parameters of these two models are the same, excluding the impacts of parameters on simulation comparison between DBH_GW and DBH_NGW.

3.4 Experiment design

To evaluate the effects of the groundwater representation on hydrological modeling, hydrological simulation with the groundwater scheme (DBH_GW) and the control experiment without groundwater consideration (DBH_NGW) are compared against observed monthly river discharge and GRACE TWS anomalies. Both experiments are run with a long

spin-up period from 1982 to 2002 to remove the uncertainties due to uncertain initial conditions, and then the model simulations were evaluated over the period from 2003 to 2014. The DBH model was run at one hour time step and at a spatial resolution of 10×10 km grids. Monthly model outputs were used to compare with observed streamflow and GRACE TWS variations. The model simulated TWS variations were calculated by the sum of simulated soil moisture W (mm), snow water equivalent S (mm), water in biomass V (mm), water in river channel R (mm), and groundwater G (mm) (G=0 in the DBH_NGW simulation):

$$TWS = W + S + V + R + G. \tag{9}$$

Four metrics are used to assess the model performance: the relative bias (BIAS), the root mean square error (RMSE), the relative root mean square error (RRMSE), and the NSC. NSC would be negative when simulated hydrological variable is very poor, and is above 0.5 for a reasonable simulation, is 1 for a perfect simulation. BIAS, RMSE, RRMSE and NSC are calculated as follows:

$$BIAS = \frac{1}{n}\sum_{i=1}^{n}(s_i - o_i)/\bar{o}; \tag{10}$$

$$RMSE = \sqrt{\frac{1}{n}\sum_{i=1}^{n}(s_i - o_i)^2}; \tag{11}$$

$$RRMSE = RMSE/\bar{o}; \tag{12}$$

$$NSC = 1 - \frac{\sum_{i=1}^{n}(s_i - o_i)^2}{\sum_{i=1}^{n}(o_i - \bar{o})^2}; \tag{13}$$

where n is the total number of time series; s_i and o_i denoted time series of observation and simulation discharge of hydrologic gauge, respectively; $\bar{o} = \sum o / n$ is the averaged value of

observation. All these scores are computed in terms of monthly values. In addition, we use the standard deviation *SD* and amplitude *A* to characterize the temporal variability of river discharge and TWS:

$$SD = \sqrt{\frac{1}{n-1}\sum_{i=1}^{n}(x_i - \bar{x})^2}\,, \tag{14}$$

$$A = x_{\max} - x_{\min}\,, \tag{15}$$

where x_i is the time series; n is the total number of time series; $\bar{x} = \sum x / n$ is the averaged value of x; $x_{\max}$ and $x_{\min}$ are the maximum and minimum value of x, respectively. A high standard deviation and amplitude value indicate large variability of the time series.

4 Results

4.1 The influence of groundwater dynamics on river discharge simulation

Figure 3(a) shows the comparisons between the DBH_GW and DBH_NGW monthly river discharge from 2003 to 2014 against observations at Tangnaihai station. The BIAS, RMSE, RRMSE and NSC of DBH_GW are -1.48%, 179m^3/s, 0.28 and 0.87, respectively; while these of DBH_NGW are 4.96%, 259m^3/s, 0.41 and 0.72, respectively. In addition, the standard deviations of DBH_GW and DBH_NGW monthly river discharge are 471 m^3/s and 642m^3/s respectively, against 491m^3/s of observations; while the amplitudes of them are 2234m^3/s and 2849m^3/s respectively, against 2442m^3/s of observations. In terms of the annual cycle of river discharge (shown in Fig. 3(b)), the BIAS, RMSE, RRMSE and NSC of DBH_GW are -1.48%, 100m^3/s, 0.16 and 0.94, respectively; while these of DBH_NGW are 4.96%, 214m^3/s, 0.33and 0.74, respectively. It is evident that all quantitative metrics have

been greatly improved by incorporating a groundwater module into DBH model, and monthly river discharge were satisfactorily reproduced by DBH model by considering groundwater dynamics. And the consideration of groundwater dynamics also decreases the inter-annual and intra-seasonal variability of river discharge. Comparing with DBH_NGW, DBH_GW is prone to yield less river discharge in summer time and more river discharge in cold season. Additionally, the significant improvement is also found in transition seasons (spring and autumn). In comparison with DBH_GW, DBH_NGW has produced a more obvious sharp decrease of streamflow in fall and more rapid increase in spring. Furthermore, Figure 4 shows the seasonal river discharge estimates derived from DBH_GW and DBH_NGW from 2003 to 2014 against observations in the upstream of the Yellow River basin, and the evaluation indices of the DBH_GW and DBH_NGW seasonal river discharge against observations are listed in Table 1 and Table 2. The result shows the simulated river discharge, after incorporating the groundwater scheme, has been improved through reducing the bias, from 61% to 9% in spring, from 29% to 9% in summer, from 14% to 4% in fall, and from 44% to 14% in winter, respectively, corresponding to the reduced biases of 52%, 20%, 10% and 30%. The most pronounced improvements are found in cold seasons when river discharge simulated by DBH_NGW exhibits clear underestimation. Moreover, DBH_GW also simulated a more reasonable inter-annual seasonal river discharge than DBH_NGW, as the RMSE, RRMSE, and (shown in Table 2) in DBH_GW are smaller than these of DBH_NGW in all seasons, especially in spring when the RMSE value in DBH_GW is less than half of that in DBH_GW. In general, groundwater representation in DBH model improves the simulation of river discharge in upstream of the Yellow River basin. This is attributed to the model framework of

DBH_GW that is more authentic than that of DBH_NGW, and the groundwater reservoir may function as a temporal buffer for river discharge and smoothes the river discharge variation by its delayed and small amplitude response to climate signal (e.g. precipitation).

4.2 The influence of groundwater dynamics on TWS simulation

Figure 5(a) shows the simulated time series of TWS anomalies by DBH_GW and by DBH_NGW in comparison with GRACE estimates from 2003 to 2014. In terms of the inter-annual variation of the TWS, Table 3 shows the NSC between simulated TWS anomalies and GRACE data, as well as the maximum, minimum, amplitude and standard deviation of TWS anomalies. NSC of DBH_GW is large than that of DBH_NGW, and the TWS maximum, minimum, amplitude, and standard deviation values simulated by DBH_GW are closer to GRACE than these by DBH_NGW. In terms of the annual cycle of monthly TWS anomalies (shown in Fig. 5(b)), the quantitative metrics (RMSE, RRMSE and NSC) of DBH_GW (6.92mm, 2.28 and 0.91, respectively) are better than that in DBH_NGW (12.5mm, 4.14, and 0.71, respectively), suggesting that the simulation considering groundwater dynamics in DBH model gives a remarkably improved agreement with GRACE data than DBH_NGW. In addition, the TWS variation simulated by DBH_NGW decreases more slowly during October to April, and increase more slowly during April to September than these by DBH_GW. It is evident that groundwater regulates the storage of the river basin by increasing TWS amplitudes and signals, especially in spring and autumn. Generally, representation of groundwater dynamics in DBH model increases the amplitudes and

variability of TWS anomalies, and shows an improved performance in TWS inter-annual and intra-seasonal variation.

Figure 6 shows the changing trend of TWS estimated from DBH_GW, DBH_NGW and GRACE. The magnitude of trend of TWS anomalies (mm/month) are 0.24±0.09, 0.16±0.07 and 0.21±0.11 (the error range is the 95% confidence bounds) for DBH_GW, DBH_NGW and GRACE, respectively. Specifically, as simulated by the DBH_GW, groundwater and surface shows a significant increasing trend with a magnitude of 0.08±0.03 mm/month and 0.16±0.08 mm/month, respectively (Fig. 6(d)), while surface water shows a significant increase with a magnitude of 0.16±0.07 mm/month by DBH_NGW. From the results, surface water storage shows almost the same changing pattern both in DBH_GW and DBH_NGW, where increasing in soil moisture is the dominant factor. Additionally, increasing trend in groundwater is an important component of total magnitude of trend in TWS, which facilitates the DBH_GW to capture the trend of GRACE TWS data. Increasing trend of TWS in the upstream of the Yellow River basin has been reported in many studies (Mo et al., 2016; Jiao et al., 2015; Zhong et al., 2009). Increasing in TWS can be motived by various factors, including an increase in precipitation and a decrease in ET. Figure S2 shows the cumulative of the DBH_GW estimates of precipitation, ET, river discharge and the cumulative precipitation minus ET (P-ET). It shows that the cumulative P-ET is above the cumulative of river discharge, especially in the wet seasons when extra water stores in soil and groundwater reservoir and TWS increase. In addition, recent studies and local observation indicated that the study region was getting warmer and wetter after 2000 as the runoff showed a significant increasing trend (Lan et al., 2012; Wang et al., 2014). Furthermore, as the ecological

protection and construction project started in the Three-River Source regions in 2005 by the Chinese government, storage in lakes extend according to report from the Qinghai Provincial Meteorological Bureau (Mo et al., 2016). Groundwater increases in the study regions has been reported in recent years. As reported by official reports from Qinghai Provincial Climate Monitoring and Assessment Centre (2009), groundwater levels started to rise in the Three-River Source regions since 2009 due to increasing precipitation and river discharge. Results from Jiao et al. (2015) indicated that the increasing trend of groundwater level was observed from groundwater wells near the study region.

4.3 Impacts of groundwater dynamics on soil moisture and ET

The comparison of monthly volumetric soil moisture content in study region between DBH_GW and DBH_NGW is shown in Fig. 7. The seasonal cycle of soil moisture is clearly represented in Fig. 7 (a). Due to more precipitation and more water infiltrates into the soil, soil moisture in wet seasons (i.e. May to October) is higher than that in dry seasons (i.e. November to April). Generally, DBH_GW tends to represent wetter soil moisture content than DBH_NGW, especially in wet seasons (shown in Fig. 7(b)). The lower boundaries of soil column are gravitational free drainage and groundwater table in DBH_NGW and DBH_GW, respectively; and the soil moisture potential difference between the third soil layer and lower boundary in DBH_NGW is obvious larger than that of DBH_GW. Therefore, gravitational free drainage in DBH_NGW produces greater leakage from the bottom layer soil than DBH_GW. In addition, the gravitational drainage is proportional to the bottom layer soil moisture (Eq.3), thus the difference of soil moisture in DBH_GW and DBH_NGW is higher in wet seasons, and reaches the most in September. Soil moisture continues recharging

groundwater reservoir and river channels in dry seasons in DBH_GW, and the soil moisture difference decreases, and almost values 0 in April.

In terms of the annual cycle of monthly mean volumetric soil moisture (shown in Fig.8), the standard deviation and amplitude of simulated by DBH_GW are larger than these of DBH_NGW, demonstrating that the groundwater reservoir have the potential to increase soil moisture storage. Groundwater representation in DBH model change the lower boundary of soil, and the accompanying change in soil moisture potential difference between the third soil layer and lower boundary will generate less soil drainage when compared with DBH_NGW, further leading to higher soil wetness. .

The comparison of monthly time series of ET between DBH_GW and DBH_NGW is shown in Fig. 9. The seasonal cycle of ET is similar to that of soil moisture. Actual ET in dry regions is mostly determined by soil moisture, and in the upstream of the Yellow River basin, DBH_GW trend to produce much wetter soil than DBH_NGW. Therefore, DBH_GW simulates much larger ET than DBH_NGW and the difference reaches the peak in September.

5 Discussions

5.1 Mechanism of groundwater dynamics on hydrological processes

The results presented in this study indicate the benefits of incorporation groundwater module in DBH model on hydrological simulation. In the upstream of the Yellow River basin, river discharge shows a significant seasonal variation with a peak in summer and a bottom in winter, consistent with the seasonal precipitation variation. The rate of groundwater flows

into streams is determined by their hydraulic connection and hydraulic head gradient. In summer, more precipitation infiltrates into soil and further stores in groundwater reservoir, thus leads to peak flow reduction and increase in TWS and water table; while in winter, due to low precipitation and frozen soil moisture in the surface layer, groundwater discharges into river channel, resulting in reasonable simulation of streamflow and TWS. Therefore, groundwater reservoir holds the groundwater in the subsurface longer and increases the memory of TWS storage, further delays and smoothes simulated river discharge. Conversely, without consideration of the groundwater, precipitation and snow melt will transform into discharge directly, leading to more sharp increase of streamflow in spring; and river discharge in winter will be underestimated due to lack of groundwater discharge. Therefore, due to its low-frequency variability and delayed response to precipitation, groundwater representation in DBH model improves the river discharge simulation both in amount and variability, agreeing with the results in previous studies (Liang et al., 2003; Vergnes & Decharme, 2012; Pokhrel et al., 2013). Groundwater dynamics in DBH model also improves the amplitude and signal in terms of the inter-annual variation and annual cycle variability of TWS like previous studies (Maxwell & Miller, 2005; Fan et al., 2007; Niu et al., 2007; Lo et al., 2008). Furthermore, increasing trend in groundwater is an important part of trend in TWS, which further leading to an improved agreement with the magnitude of GRACE TWS changing trend.

5.2 Uncertainties in GRACE TWS estimates

The uncertainty of GRACE derived TWS estimates is still a key issue. Rodell & Famiglietti (1999) concluded that the variations of TWS would likely be detected depending

on the size of the study region and the magnitude of the TWS variations (e.g. area above 2000,000km^2 and TWS variation more than a few millimeters). Wahr et al.(2006) estimated the uncertainties in the GRACE estimates with a 750-km smoothing radius, and results showed that the error near the polos (about 8mm) are smaller than that at low latitudes (about 26mm), and the error will decrease as the test radius increase. Here we assess the uncertainty in the GRACE estimates in the upstream of the Yellow River basin using the method of Landerer & Swenson (2012). In brief, the total error in study region is obtained by summing leakage and measurement errors in quadrature:

$$Err\_tot = \sqrt{(Err\_measure)^2 + (Err\_leakage)^2} \quad ; \qquad (16)$$

Leakage and measurement errors at regional level were calculated based on the error fields provided by GRACE Tellus data. As a result of the spatial correlations of the errors in gridded scale, the error covariance (*cov*) is taken into consideration in calculation of regional error:

$$\mathrm{cov}(i, j) = Err_i * Err_j * \exp(\frac{-d_{ij}^2}{2d_0^2}) ; \qquad (17)$$

Where Err_i and Err_j are the standard deviations of the uncertainty estimates for grid points *i* and *j*; d_{ij} is the distance between two grid points, and d_0 is a decorrelation-length which is set to 100km for leakage error and 300km for measurement error. Then error variance of a regional TWS estimates (*Err_region*) is calculated as:

$$Err\_region = \sum_{i=1}^{n}\sum_{j=1}^{n} w_i w_j \,\mathrm{cov}(i, j) ; \qquad (18)$$

where w_i and w_j are the area weights to the region for grid i and j, respectively. From the analysis, the measurement error and leakage error of GRACE estimates are 11.1mm and 22.1mm, respectively, and the total error is 24.4mm in the upstream of the Yellow River basin. To further analyze the uncertainty of GRACE estimates, the standard deviation of the monthly GRACE TWS are calculated (Figure S3). The amplitude of annual cycle of GRACE TWS estimates is 64.4mm (after de-trending), and the standard deviations of the monthly GRACE TWS are with the range 11-20mm. In general, in spite that the regional error (24.4mm) is beyond the accuracy (21mm), low standard deviations of the monthly GRACE TWS and high amplitude of annual cycle indicate that TWS variation in the upstream of the Yellow River basin is detectable by GRACE estimates.

5.3 Limitations and future works

We acknowledge that there are still some deficiencies appearing in the simulations. For example, the simulated river discharge is over-simulated in high flow seasons (e.g. June-August) and under-estimated in in autumn (i.e. October and November). In spite of the reasonable simulation of TWS by DBH_GW, the seasonal amplitude of TWS is smaller than GRACE estimation, especially in high flow seasons (e.g. July-October). These deficiencies in hydrological simulation can be attributed to multi reasons, such as the uncertainties in climate forcing, model structure and parameters (Alkama et al., 2010; Vergnes & Decharme, 2012). In this part, we will discuss the limitations and future works of the groundwater module of the DBH model.

Firstly, only a single layer is introduced below the soil column in the groundwater module, and groundwater is treated as a reservoir that regulates hydrological processes. Intermediate zone and groundwater aquifer constitute a complex system which is poorly represented by the simple one-layer groundwater scheme in the DBH model. In fact, groundwater stores in unconfined aquifer which can be presented by multiple layers and physically based distributed dynamic groundwater model can well represent the groundwater flows (Wendland et al., 2004; Niu et al., 2007; Tian et al., 2012), and deep soil also play an important role in hydrological processes (Le Vine et al., 2016). Water stores in the intermediate zone between unsaturated soil and groundwater is of great significance in TWS variation (Rodell & Famiglietti, 2001), and without consideration of intermediate zone could result in underestimation of TWS. Furthermore, the interaction between confined aquifer and surface water is considerable, and water storing in confined aquifer has been proved to be a great part of total TWS (de Graaf et al., 2017). Only vertical water exchanges between groundwater and surface water are considered in this study, but neglecting sub-grid groundwater flow and lateral flow in soil which has significant impacts on hydrological processes (Tian et al., 2012). Furthermore, groundwater depth in DBH model is converted by the groundwater storage variation, while a physical mechanism based water table parameterization is still lack, which could have a direct impact on the simulated water table and then affect baseflow simulation. Additionally, groundwater withdrawal for anthropogenic activity, which has been proved to be of great significance to water cycle (Wada et al., 2010; Döll et al., 2014; Leng et al., 2014; Pokhrel et al., 2015), will be integrated into DBH model in the future. In general, future works would be conducted for enhancing the model capability, and a more realistic

groundwater model which can well represent the three-way interactions among river water, groundwater, and land surface processes is expected.

6 Conclusions

In the study, a groundwater scheme, considering the interactions of surface water and groundwater, is incorporated into the DBH model. The groundwater scheme is parameterized on the basis of a conceptual groundwater reservoir with the dynamic representation of the interactions among soil moisture, groundwater, and river. Two numerical experiment are conducted in the upstream of the Yellow River basin with one based on a default model without groundwater dynamic (DBH_NGW), and the other with groundwater module active (DBH_GW). The main conclusions are summarized as follows:

1. River discharge simulation is greatly improved with incorporation of groundwater dynamics in the DBH model mainly through reducing the bias in the seasonality. Specifically, DBH_GW simulates less streamflow in summer and more river discharge in cold season; while DBH_NGW produces a sharp decrease of streamflow in fall and more rapid increase in spring when compared with DBH_GW. Consideration of groundwater module in DBH model leads to decrease in the variability of total river discharge, inter-annual variation and seasonal cycle of river discharge, which matches better with observations than the default model.

2. Comparing the TWS variation simulated by two experiments (i.e. DBH_GW and DBH_NGW) and GRACE estimates, it is found that DBH_GW better reproduced the change pattern of TWS against GRACE data than DBH_NGW, especially in terms of the inter-annual and intra-seasonal variability. Furthermore, the TWS without groundwater

(DBH_NGW) decreases more slowly during cold season and increase more slowly in warm season when compared with DBH_GW. Additionally, changing trend in groundwater is an important component of trend in TWS, and consideration of dynamics of groundwater will further leads to an improved agreement of simulated TWS with GRACE in terms of the magnitude of TWS changing trend.

3. DBH_GW simulates less drainage in soil and the simulated soil moisture of DBH_GW is wetter than that of DBH_NGW, especially in wet season, which subsequently affects the simulated ET because the calculation of ET is based on soil moisture.

We acknowledge that the conclusions summarized in this study are restricted the specific model in the case study region, and there are still many limitations and deficiencies in the groundwater module. Thus, a global-scale study should be pursued in the future to evaluate whether the findings of this study would hold in other regions, and more efforts will be devoted to enhancing the model capability by considering three-way interactions among river water, groundwater, and land surface processes, and importantly, the sub-grid groundwater flow and lateral flow will be also coupled in groundwater module in the future.

Acknowledgements

Funding for this research was provided by the National Natural Science Foundation of China (41730645, 41790424, and 41425002), and the Strategic Priority Research Program of

Chinese Academy of Sciences (XDA20060402). Min-Hui Lo was supported by the funding of MOST-104-2923-M-002-002-MY4.

References

Alcamo, J., DÖll, P., Henrichs, T., Kaspar, F., Lehner, B., Rosch, T., & Siebert, S. (2003). Development and testing of the WaterGAP 2 global model of water use and availability. *Hydrological Sciences Journal, 48*(3), 317-337.

Alkama, R., Decharme, B., Douville, H., Becker, M., Cazenave, A., Sheffield, J., . . . Moigne, P. L. (2010). Global Evaluation of the ISBA-TRIP Continental Hydrological System. Part I: Comparison to GRACE Terrestrial Water Storage Estimates and In Situ River Discharges. *Journal of Hydrometeorology, 11*(3), 583-600.

Arora, V. K., & Boer, G. J. (1999). A variable velocity flow routing algorithm for GCMs. *Journal of Geophysical Research Atmospheres, 104*(D24), 30965–30979.

Cherkauer, K. A., & Lettenmaier, D. P. (1999). Hydrologic effects of frozen soils in the upper Mississippi River basin. *Journal of Geophysical Research Atmospheres, 104*(D16), 19599-19610.

Childs, E. C. (1971). Drainage of Groundwater Resting on a Sloping Bed. *Water Resources Research, 7*(7), 1256-1263.

Cong, Z., Yang, D., Gao, B., Yang, H., & Hu, H. (2009). Hydrological trend analysis in the Yellow River basin using a distributed hydrological model. *Water Resources Research, 45*(7).

Döll, P., Fritsche, M., Eicker, A., & Schmied, H. M. (2014). Seasonal Water Storage Variations as Impacted by Water Abstractions: Comparing the Output of a Global Hydrological Model with GRACE and GPS Observations. *Surveys in Geophysics, 35*(6), 1311-1331.

Davie, J., Falloon, P., Kahana, R., Dankers, R., Betts, R., Portmann, F., . . . Masaki, Y. (2013). Comparing projections of future changes in runoff from hydrological and biome models in ISI-MIP. *Earth System Dynamics, 4*, 359-374.

Decharme, B., Alkama, R., Douville, H., Becker, M., & Cazenave, A. (2010). Global Evaluation of the ISBA-TRIP Continental Hydrological System. Part II: Uncertainties in River Routing Simulation Related to Flow Velocity and Groundwater Storage. *Journal of Hydrometeorology, 11*(3), 601-617.

de Graaf, I. E. M., van Beek, R. L. P. H., Gleeson, T., Moosdorf, N., Schmitz, O., Sutanudjaja, E. H., and Bierkens, M. F. P.: (2017). A global-scale two-layer transient groundwater model: Development and application to groundwater depletion, *Advances in Water Resources*, 102, 53-67, https://doi.org/10.1016/j.advwatres.2017.01.011.

Fan, Y., Li, H., & Miguezmacho, G. (2013). Global patterns of groundwater table depth. *Science, 339*(6122), 940-943.

Fan, Y., Miguez-Macho, G., Weaver, C. P., Walko, R., & Robock, A. (2007). Incorporating water table dynamics in climate modeling: 1. Water table observations and equilibriu

water table simulations. *Journal of Geophysical Research Atmospheres, 112*(112), 676-684.

Franchini, M., & Pacciani, M. (1991). Comparative analysis of several conceptual rainfall-runoff models. *Journal of Hydrology, 122*(s 1–4), 161-219.

Hattermann, F., Krysanova, V., Gosling, S., Dankers, R., Daggupati, P., Donnelly, C., . . . Buda, S. (2016). Cross‐scale intercomparison of climate change impacts simulated by regional and global hydrological models in eleven large river basins. *Climatic Change*, 1-16.

Information Center of Water Resources. (2003-2014). *Hydrological Year Book (in Chinese)*. Beijing: Information Center of Water Resources, Ministry of Water Resources of the People's Republic of China.

Lam, A., Karssenberg, D., van den Hurk, B. J. J. M., & Bierkens, M. F. P. (2011). Spatial and temporal connections in groundwater contribution to evaporation. *Hydrology & Earth System Sciences Discussions, 15*(8), 2621-2630.

Landerer, F., & Swenson, S. (2012). Accuracy of scaled GRACE terrestrial water storage estimates. *Water Resources Research, 48*(4).

Leng, G., Huang, M., Tang, Q., Gao, H., & Leung, L. R. (2014). Modeling the Effects of Groundwater-Fed Irrigation on Terrestrial Hydrology over the Conterminous United States. *Journal of Hydrometeorology, 15*(3), 957-972.

Liang, X., Lettenmaier, D. P., Wood, E. F., & Burges, S. J. (1994). A simple hydrologically based model of land surface water and energy fluxes for general circulation models. *Journal of Geophysical Research Atmospheres, 99*(D7), 14415–14428.

Liang, X., Xie, Z., & Huang, M. (2003). A new parameterization for surface and groundwater interactions and its impact on water budgets with the variable infiltration capacity (VIC) land surface model. *Journal of Geophysical Research Atmospheres, 108*(D16), 832-833.

Lin, Y.-H., Lo, M.-H., & Chou, C. (2016). Potential negative effects of groundwater dynamics on dry season convection in the Amazon River basin. *Climate Dynamics, 46*(3-4), 1001-1013.

Liu, X., Tang, Q., Voisin, N., & Cui, H. (2016). Projected impacts of climate change on hydropower potential in China. *Hydrology and Earth System Sciences, 20*, 3343-3359.

Lo, M. H., Famiglietti, J. S., Yeh, J. F., & Syed, T. H. (2010). Improving parameter estimation and water table depth simulation in a land surface model using GRACE water storage and estimated base flow data. *Water Resources Research, 46*(W05517), 1-15.

Lo, M. H., Yeh, J. F., & Famiglietti, J. S. (2008). Constraining Water Table Depth Simulations in a Land Surface Model Using Estimated Baseflow. *Advances in Water Resources, 31*(12), 1552-1564.

Maxwell, R. M., & Miller, N. L. (2005). Development of a Coupled Land Surface and Groundwater Model. *Journal of Hydrometeorology, 6*(3), 233.

Miguez-Macho, G., & Fan, Y. (2012). The role of groundwater in the Amazon water cycle: 2. Influence on seasonal soil moisture and evapotranspiration. *Journal of Geophysical Research Atmospheres, 117*(D15), 156-169.

Myneni, R. B., Ramakrishna, R., Nemani, R., & Running, S. W. (1997). Estimation of global leaf area index and absorbed par using radiative transfer models. *IEEE Transactions on Geoscience & Remote Sensing, 35*(6), 1380-1393.

New, M., Hulme, M., & Jones, P. (2000). Representing Twentieth-Century Space-Time Climate Variability. Part II: Development of 1901-96 Monthly Grids of Terrestrial Surface Climate. *Journal of Climate, 13*(13), 2217-2238.

Niu, G. Y., Yang, Z. L., Dickinson, R. E., Gulden, L. E., & Su, H. (2007). Development of a simple groundwater model for use in climate models and evaluation with Gravity Recovery and Climate Experiment data. *Journal of Geophysical Research Atmospheres, 112*(D7), 277-287.

Pokhrel, Y. N., Fan, Y., Miguez-Macho, G., Yeh, J. F., & Han, S. C. (2013). The role of groundwater in the Amazon water cycle: 3. Influence on terrestrial water storage computations and comparison with GRACE. *Journal of Geophysical Research Atmospheres, 118*(8), 3233-3244.

Pokhrel, Y. N., Koirala, S., Yeh, P. J. F., Hanasaki, N., Longuevergne, L., Kanae, S., & Oki, T. (2015). Incorporation of groundwater pumping in a global Land Surface Model with the representation of human impacts. *Water Resources Research, 51*(1), 78-96.

Rodell, M., & Famiglietti, J. S. (2001). An analysis of terrestrial water storage variations in Illinois with implications for the Gravity Recovery and Climate Experiment (GRACE). *Water Resources Research, 37*(5), 1327–1339.

Sellers, P. J. (1986). Simple biosphere model (SiB) for use within general circulation models. *Journal of the Atmospheric Sciences, 43*(6), 505-531.

Sellers, P. J., Randall, D. A., Collatz, G. J., Berry, J. A., Field, C. B., Dazlich, D. A., . . . Bounoua, L. (1996). A Revised Land Surface Parameterization (SiB2) for Atmospheric GCMS. Part I: Model Formulation. *Journal of Climate, 9*(4), 676-705.

Shiklomanov, I. A., & Rodda, J. C. (2004). World Water Resources at the Beginning of the Twenty-First Century. *International Hydrology, 13*.

Tang, Q., & Oki, T. (2016). *Terrestrial Water Cycle and Climate Change: Natural and Human-Induced Impacts* (Vol. 221): John Wiley & Sons.

Tang, Q., Oki, T., & Kanae, S. (2006). A distributed biosphere hydrological model (DBHM) for lager river basin. *Annual Journal of Hydraulic Engineering JSCE, 50*, 37-42.

Tang, Q., Oki, T., Kanae, S., & Hu, H. (2007). The Influence of Precipitation Variability and Partial Irrigation within Grid Cells on a Hydrological Simulation. *Journal of Hydrometeorology, 8*(3), 499.

Tang, Q., Oki, T., Kanae, S., & Hu, H. (2008). A spatial analysis of hydro‐climatic and vegetation condition trends in the Yellow River basin. *Hydrological processes, 22*(3), 451-458.

Tian, W., Li, X., Cheng, G.-D., Wang, X.-S., and Hu, B. X.(2012). Coupling a groundwater model with a land surface model to improve water and energy cycle simulation, *Hydrol. Earth Syst. Sci.*, 16, 4707-4723, https://doi.org/10.5194/hess-16-4707-2012.Todini, E. (1988). Rainfall-runoff modeling—Past, present and future. *Journal of Hydrology, 100*(1–3), 341-352.

Towner, G. D. (1975). Drainage of groundwater resting on a sloping bed with uniform rainfall. *Water Resources Research, 11*(1), 144-147.

Vergnes, J. P., & Decharme, B. (2012). A simple groundwater scheme in the TRIP river routing model: global off-line evaluation against GRACE terrestrial water storage estimates and observed river discharges. *Hydrology & Earth System Sciences Discussions, 9*(7), 8213-8256.

Wada, Y., Beek, L. P. H. V., Kempen, C. M. V., Reckman, J. W. T. M., Vasak, S., & Bierkens, M. F. P. (2010). Global depletion of groundwater resources. *Geophysical Research Letters, 37*(20), 114-122.

Wendland, E., Rabelo, J., & Roehrig, J. (2004). Guarani Aquifer System - The Strategical Water Source In South America. *Geologiadelparaguay Com*.

Yang, D., Sun, F., Liu, Z., Cong, Z., & Lei, Z. (2006). Interpreting the complementary relationship in non-humid environments based on the Budyko and Penman hypotheses. *Geophysical Research Letters, 33*(18), 122-140.

Yeh, P. J. F., & Eltahir, E. A. B. (2005). Representation of Water Table Dynamics in a Land Surface Scheme. Part I: Model Development. *Journal of Climate, 18*(12), 1861-1880.

Zeng, Y., Xie, Z., & Zou, J. (2016). Hydrologic and climatic responses to global anthropogenic groundwater extraction. *Journal of Climate*(2016).

Zhang, X. J., Tang, Q., Pan, M., & Tang, Y. (2014). A Long-Term Land Surface Hydrologic Fluxes and States Dataset for China. *Journal of Hydrometeorology, 15*(5), 2067-2084.

Zhu, Z., Bi, J., Pan, Y., & Ganguly, S. (2013). Global Data Sets of Vegetation Leaf Area Index (LAI)3g and Fraction of Photosynthetically Active Radiation (FPAR)3g Derived from Global Inventory Modeling and Mapping Studies (GIMMS) Normalized Difference Vegetation Index (NDVI3g) for the Period 1981 to 20. *Remote Sensing, 5*(2), 927-948.

Table 1 Comparison between the DBH_GW and DBH_NGW mean seasonal river discharge from 2003 to 2014 against observations at Tangnaihai station

Season	R1*	R2	Ro	E1=|R1-Ro|/Ro	E2=|R2-Ro|/Ro
Nov-Jan	259	170	302	14%	44%
Feb-Apr	226	98	249	9%	61%
May-Jul	992	1172	910	9%	29%
Aug-Oct	1028	1225	1078	4%	14%

*R1 and R2 are the mean seasonal river discharge from 2003 to 2014 simulated by DBH_GW and DBH_NGW (m^3/s), respectively; Ro is the observation data (m^3/s); E1 and E2 are the relative error produced by DBH_GW and DBH_NGW, respectively.

Table 2 RMSE, RRMSE, and NSC values of simulated multi-annual seasonal river discharge variations against observations

	Nov-Jan		Feb-Apr		May-Jul		Aug-Oct	
	GW	NGW	GW	NGW	GW	NGW	GW	NGW
RMSE(m^3/s)	70.5	138.3	47.1	156.1	172	289.9	157.6	195.2
RRMSE	0.23	0.44	0.19	0.63	0.19	0.32	0.14	0.18
NSC	0.25	-1.91	0.19	-7.8	0.65	0.01	0.65	0.46

Table 3 The NSC between simulated TWS anomalies and GRACE data, and the minimum value, maximum value, amplitude and standard deviation of them

	NSC	standard deviation(mm)	Minimum TWS(mm)	Maximum TWS(mm)	Amplitude (max-min)(mm)
DBH_GW	0.73	25.35	-63.72	76.66	140.38
DBH_NGW	0.63	16.65	--42.85	61.99	104.84
GRACE	*	28.34	-69.11	72.78	141.89

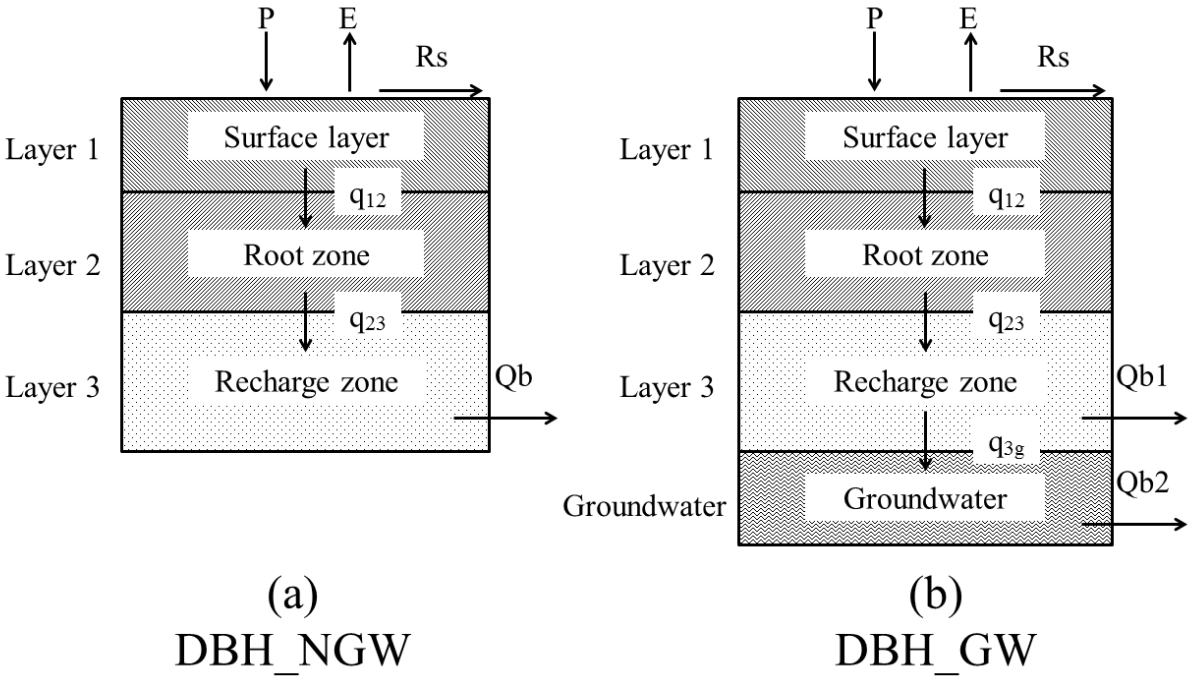

Figure 1: A schematic representation of (a) DBH_GW and (b) DBH_NGW of the water fluxes in soil layers.

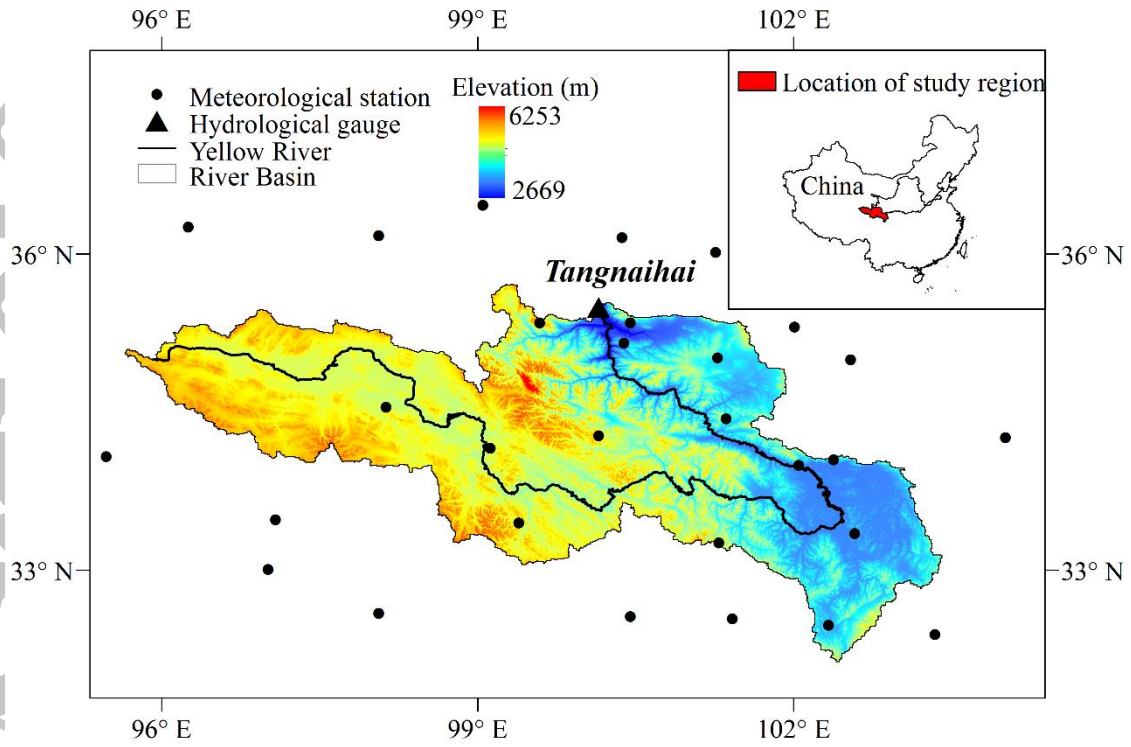

Figure 2: The upstream of the Yellow River basin.

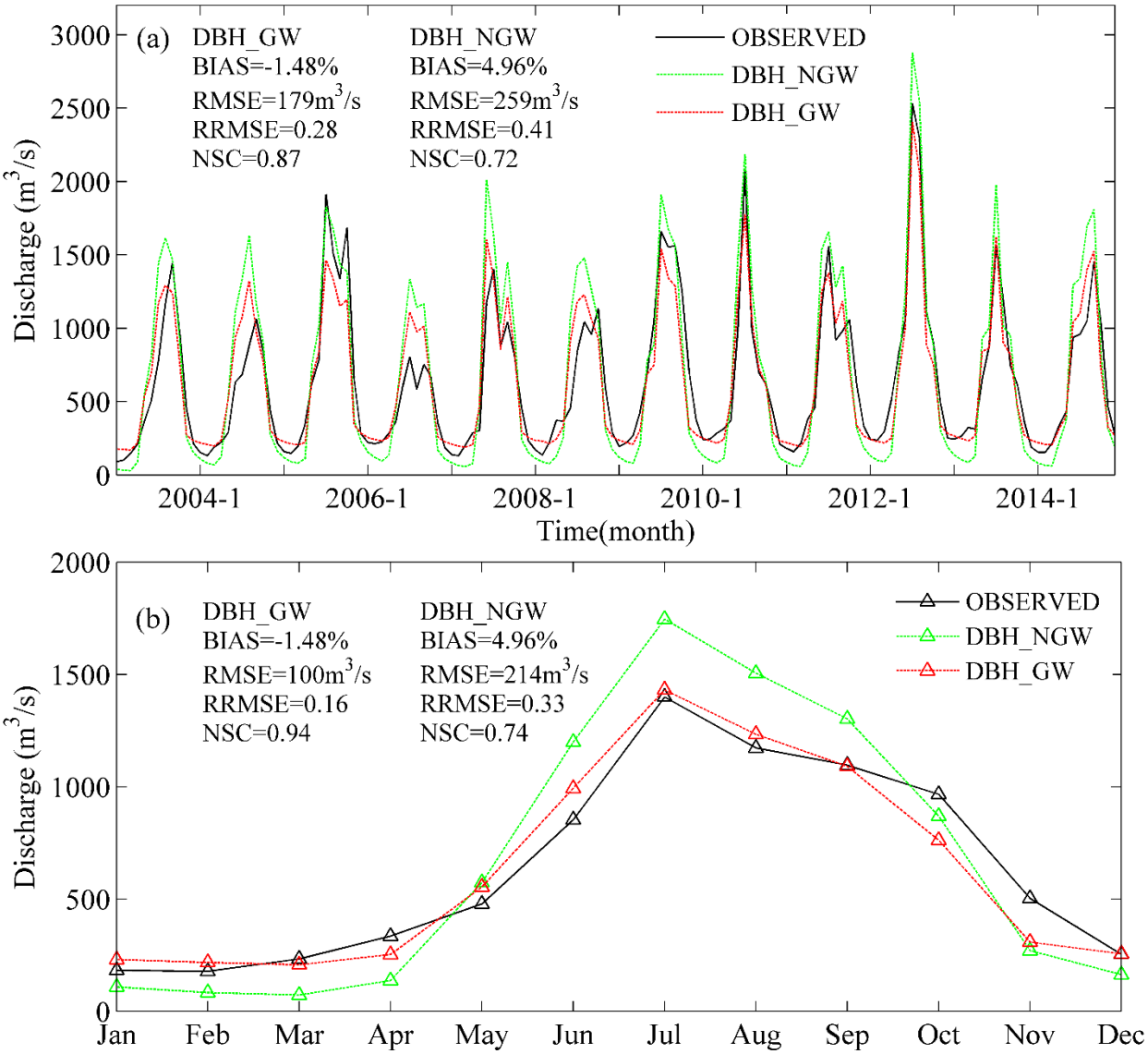

Figure 3: Comparison between the DBH_GW and DBH_NGW in (a) monthly river discharge variation and (b) multi-year monthly mean river discharge from 2003 to 2014 against observations at Tangnaihai station.

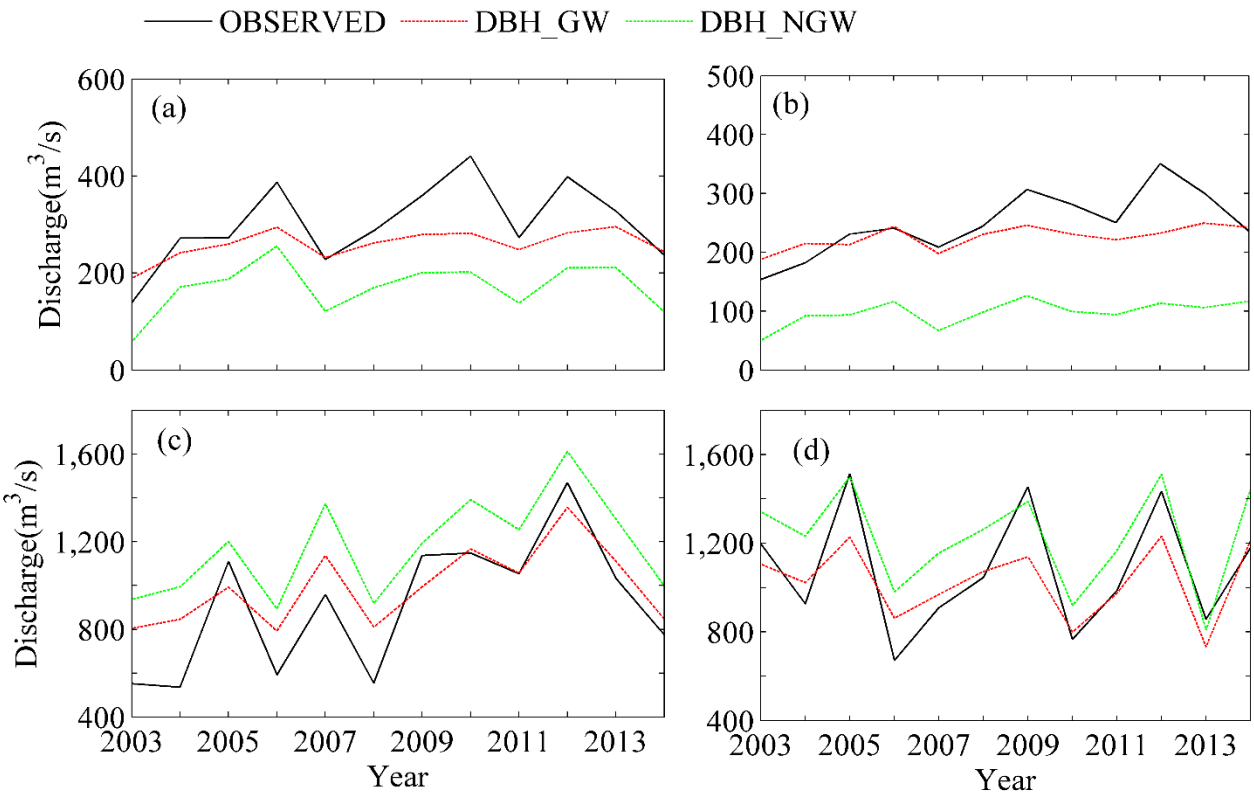

Figure 4: Seasonal river discharge evaluation from 2003 to 2014 against observations in the upstream of the Yellow River basin: (a) NDJ: from November to January next year; (b) FMA: from February to April; (c) MJJ: from May to July; (d) ASO: from August to October.

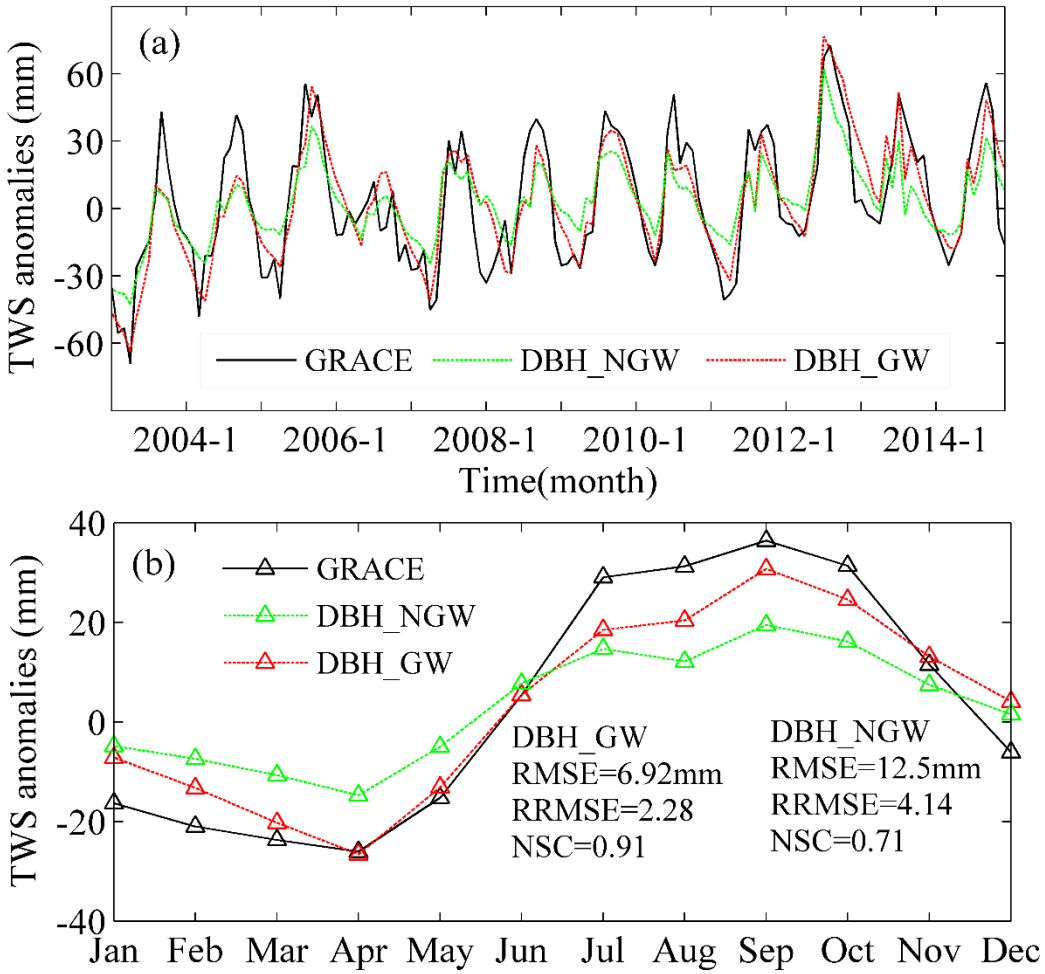

Figure 5: (a) The simulated anomalies of the TWS by DBH_GW (water in surface ponding and canopy, soil water, groundwater and snow) and by DBH_NGW (water in surface ponding and canopy, soil water and snow) in comparison with GRACE data from 2003 to 2014; (b) the simulated monthly mean anomalies of the TWS by DBH_GW and by DBH_NGW in comparison with GRACE data from 2003 to 2014.

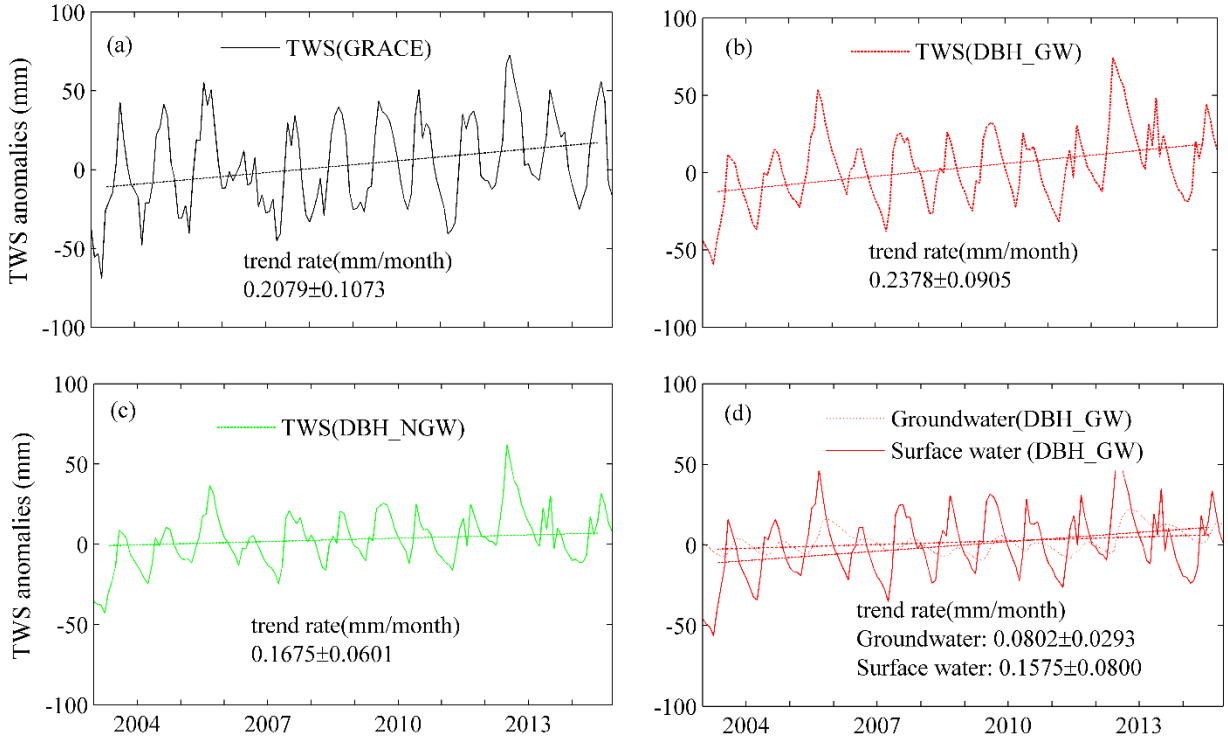

Figure 6: TWS variation and trend from 2003 to 2014: (a) TWS anomalies of GRACE data; (b) TWS anomalies of DBH_GW; (c) TWS anomalies of DBH_NGW; (d) groundwater and surface water anomalies of DBH_GW.

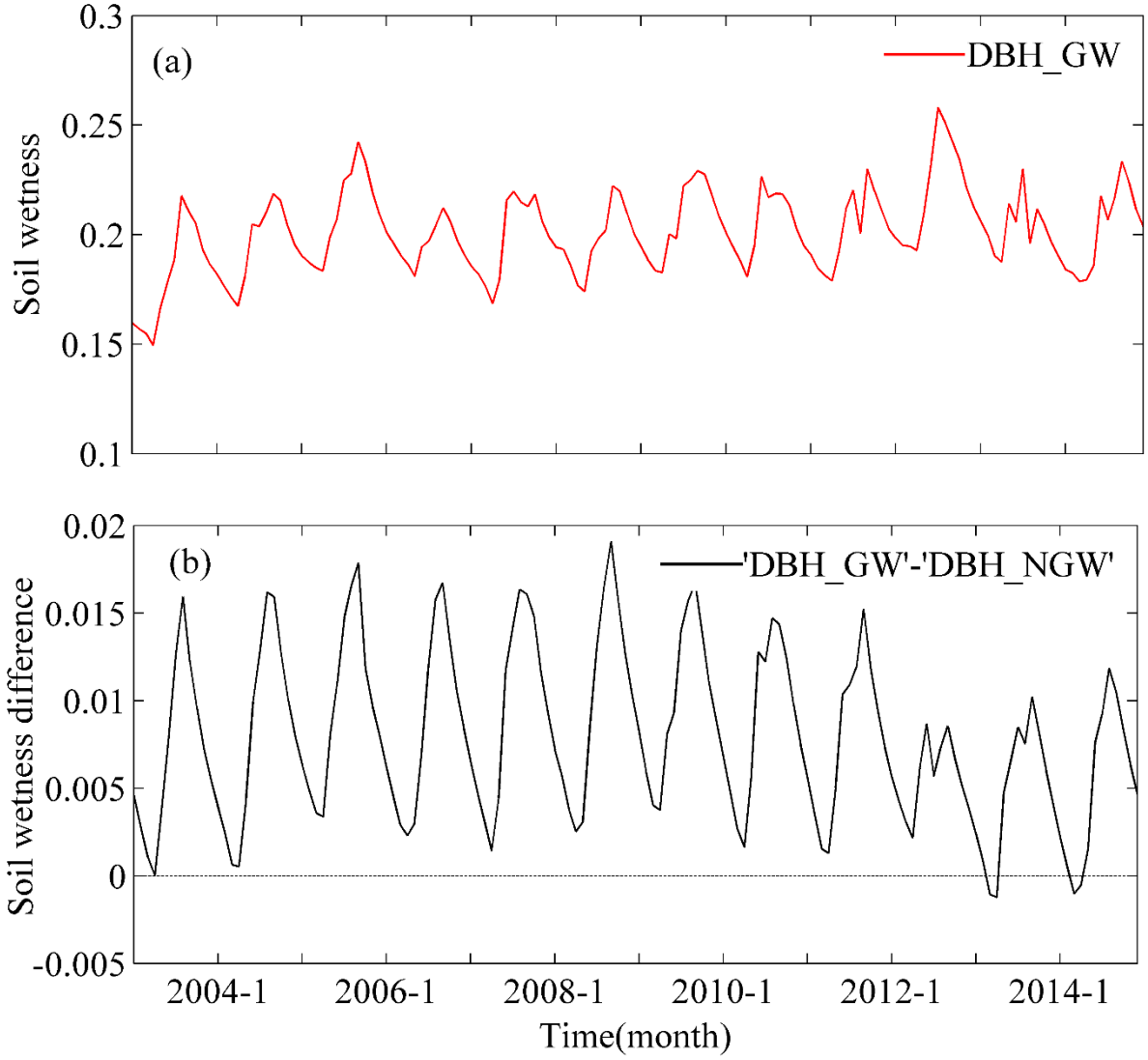

Figure 7: Comparison of monthly time series of volumetric soil moisture content in study region between DBH_GW and DBH_NGW: (a) monthly soil moisture time series simulated by DBH_GW from 2003 to 2014; and (b) differences of monthly soil moisture between DBH_GW and DBH_NGW during the period 2003-2014.

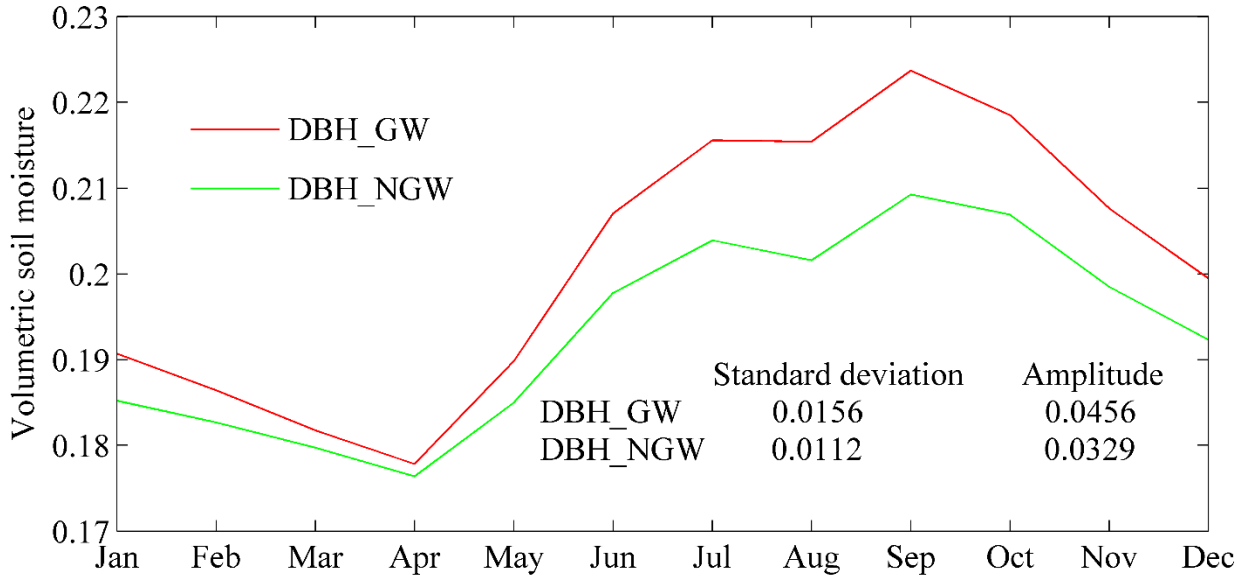

Figure 8: Comparison of annual cycle of volumetric soil moisture simulated by DBH_GW and DBH_NGW.

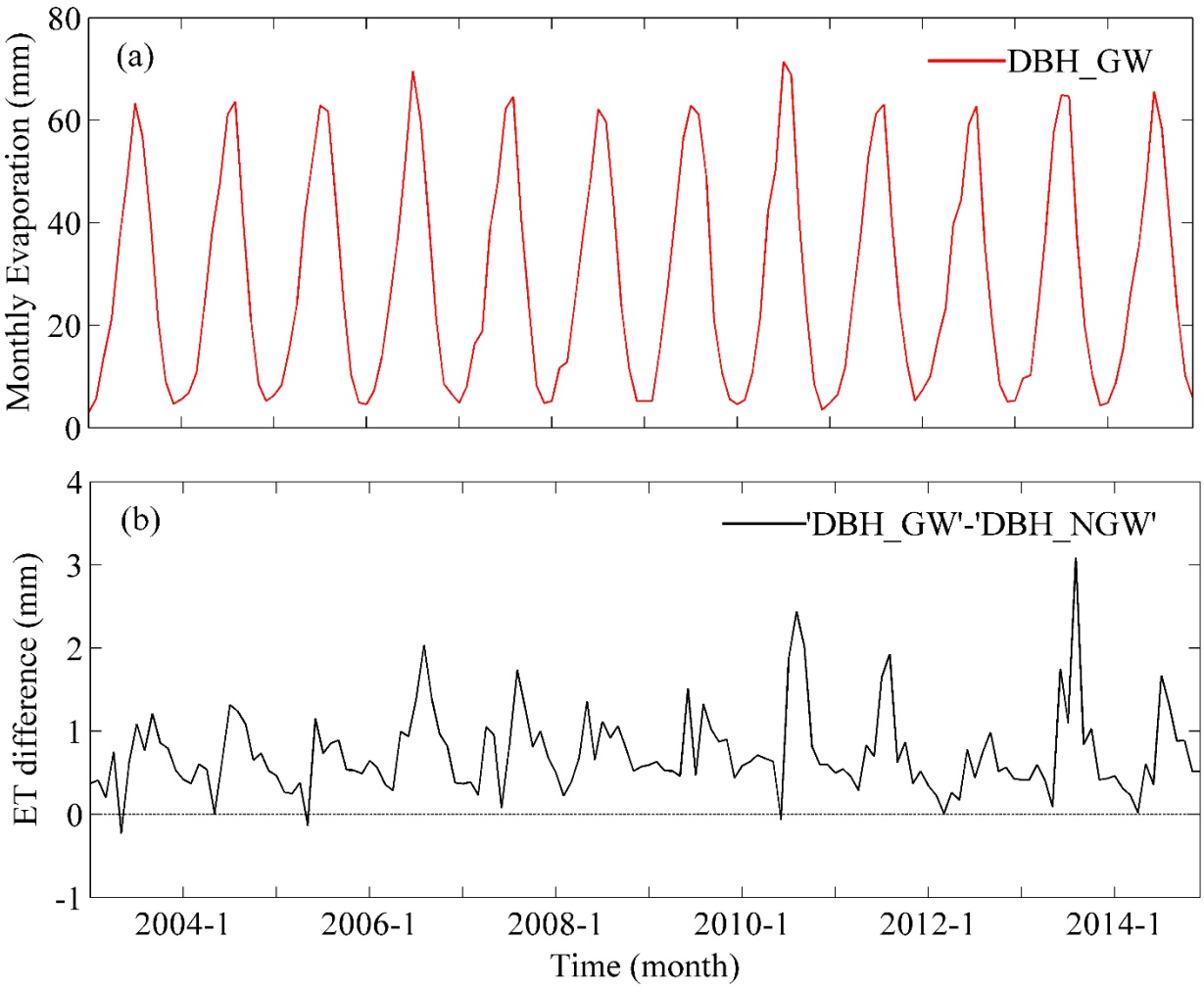

Figure 9: Comparison of monthly time series of ET in study region between DBH_GW and DBH_NGW: (a) monthly ET time series simulated by DBH_GW from 2003 to 2014; and (b) differences of monthly ET between DBH_GW and DBH_NGW during the period 2003-2014.